

DRAFT VERSION FEBRUARY 13, 2026

Typeset using L^AT_EX **manuscript** style in AASTeX7.0.1

Tidal triggers and the predictability of solar activity

FRANK STEFANI,¹ GERRIT M. HORSTMANN,¹ GEORGE MAMATSASHVILI,^{1,2} AND TOM WEIER¹

¹*Institute of Fluid Dynamics, Helmholtz-Zentrum Dresden-Rossendorf, Bautzner Landstrasse 400, 01328 Dresden, Germany*

²*Abastumani Astrophysical Observatory, Mount Kanobili, Abastumani 0301, Georgia*

ABSTRACT

Magneto-Rossby waves in the solar tachocline are currently considered to be one of the main determinants of solar activity. In particular, they can give rise to the quasi-biennial oscillation (QBO). The latter was recently shown to be dominated by a phase-stable period of around 1.7 years. By analyzing 72 ground-level enhancement (GLE) events and 37 S-flares, we determine that this period is close to 1.723 years. This, in turn, is the dominant beat between the periods of the spring tides of the tidally dominant planets Venus, Earth, and Jupiter, which are suspected to synchronize not only the QBO, but also the 11.07-year Schwabe cycle. We demonstrate that recent events, such as the solar storm of 2024 May 10 and the strong X-flare of 2026 February 1, align well with maxima of the tidal forcing. By contrast, the Carrington event (1859 September 1) does not fit this pattern.

Keywords: Sun: interior - Sun: magnetic fields - Sun: oscillations

1. INTRODUCTION

The importance of Rossby waves for terrestrial weather systems and their predictability has been recognized for almost a century (Rossby 1939; Pedlosky 1987). However, Rossby waves may also play a key role in space weather which is governed by solar activity (Zaqarashvili et al. 2010a,b; Dikpati 2012; Márquez-Artavia et al. 2017; Dikpati et al. 2018; Zaqarashvili et al. 2021). As first discussed by

Zaqarashvili et al. (2010a), they can naturally explain the Sun’s quasi-biennial oscillations (QBO). Using the shallow-water magnetohydrodynamic approximation, these authors demonstrated that the interaction between differential rotation and a toroidal magnetic field exceeding 10^5 G can lead to the instability of magneto-Rossby waves with a period of approximately two years. Later on, Raphaldini & Raupp (2015) argued that the dynamics of a resonant triad of magneto-Rossby waves could lead to periodically changing wave amplitudes with periods comparable to the dominant 11-year Schwabe cycle.

In addition to the huge energy reservoirs provided by differential rotation and toroidal magnetic fields, there are other sources that can cause neutrally stable Rossby waves to become unstable. One of them was recently discussed by Horstmann et al. (2023) who considered the tidal forces exerted by the revolving planets on the Sun. When forced by realistic-amplitude tides, magneto-Rossby waves were shown to acquire velocities in the order of m/s or larger, depending on a damping parameter whose precise value is, however, still unknown. Based on this result, it was demonstrated by Stefani et al. (2024) that the two-planet spring tides of Venus-Jupiter (with period 118 days), Earth-Jupiter (199 days), and Venus-Earth (292 days) lead to a beat period of 11.07 years which corresponds remarkably well to the Schwabe cycle. Another beat period of 1.723 years was found to agree very precisely with the dominant period underlying the occurrence of ground level enhancement (GLE) events (Stefani et al. 2025). This work also confirmed the remarkable finding of Velasco Herrera et al. (2018) that those GLE events exhibit phase stability over nearly six solar cycles.

In view of this phase stability, and the time lag of approximately 1.7 years between the solar storm of 2024 May 10 and the strong X-class flare of 2026 February 1, it is tempting to take a closer look into the potential predictability of space weather events³. This is precisely the subject matter of the present paper. It goes beyond our previous work (Stefani et al. 2025) in two respects. Firstly, in

³ When asked by spaceweather.com about the potential impact of the upcoming Venus-Earth-Jupiter alignment on solar activity, one of us (F.S.) made on 2026 January 7 the following prediction: “If the alignment excites magneto-Rossby waves as our model predicts, we might expect a higher probability of strong solar activity 40 to 60 days from now” (<https://spaceweather.com/archive.php?view=1&day=07&month=01&year=2026>). Unfortunately, due to a bug in the underlying code, this estimate was off by one month and should have read “10 to 30 days from now”, which would have included the 2026 February 1 event. Further details on that issue will be discussed below.

addition to the 72 GLE events, we will analyze a series of 37 S-class events for which we will also find phase stability with a dominant period that is very close to that of the GLE events.

Secondly, we will compute the correlations of a merger of GLE and S-flare data not only with a single cosine function, but also with the actual beat signal resulting from the superposition of the three underlying tidal triggers. We will see that a significant portion of the events correspond with the peaks of that beat signal. This particularly applies to the solar events of 2024 May 10 and 2026 February 1.

While these results support the validity for the validity of a close link between tidally triggered magneto-Rossby waves and increased solar activity, we will also demonstrate that the Carrington event of 1859 September 1 does not fit into the picture.

The paper will close with some conclusions and an outlook on further work.

2. GROUND LEVEL ENHANCEMENT EVENTS

In this section we revisit the GLE events that were analyzed previously by [Velasco Herrera et al. \(2018\)](#) and [Stefani et al. \(2025\)](#). These sporadic events are related to relativistic solar particles that produce air showers, the effects of which can be measured at ground level by a network of detectors. Table 1 and Figure 3 of [Velasco Herrera et al. \(2018\)](#) revealed that the 56 considered GLE events occurred preferentially in the positive phase of an oscillation with a period of 1.73 years which indeed points to a clocked process that was phase stable over approximately six solar cycles.

In [Stefani et al. \(2025\)](#) we had re-analyzed the sequence of GLE events, updating it from the 56 events used in [Velasco Herrera et al. \(2018\)](#) to the 71 events provided by the database of neutron monitor count rates at <https://gle.oulu.fi>. To precisely determine the best-fit period, we replaced the inverse wavelet method of [Velasco Herrera et al. \(2018\)](#) by computing the correlation coefficient $\text{Corr} = 1/71 \sum_{i=1}^{71} \cos(2\pi t_i/T_0 + \varphi_0)$ of the 71 GLE instants t_i , using cosine functions with variable periods T_0 and phases φ_0 . While Corr is not exactly Pearson's empirical correlation coefficient, it shares with it the main property of lying between -1 and 1. The latter value only occurs when the events and the cosine's maxima are perfectly aligned. Figure 8 of [Stefani et al. \(2025\)](#) showed a maximum correlation of 0.2964 for a period of 629.85 days, which corresponds to 1.724 years. This

Table 1. Numbers, dates in the format YYYY/MM/DD, and days elapsed since 1955/12/31 of the 72 GLE events considered here. Note the beginning of the numbering with 5, and the missing event 17, according to the dataset provided at <https://gle.oulu.fi> .

Nr	Date	Days	Nr	Date	Days	Nr	Date	Days
5	1956/02/23	54	30	1977/11/22	7997	54	1992/11/02	13456
6	1956/08/30	243	31	1978/05/07	8163	55	1997/11/06	15286
7	1959/07/17	1294	32	1978/09/23	8302	56	1998/05/02	15463
8	1960/05/04	1586	33	1979/08/21	8634	57	1998/05/06	15467
9	1960/09/03	1708	34	1981/04/10	9232	58	1998/08/24	15577
10	1960/11/12	1778	35	1981/05/10	9262	59	2000/07/14	16267
11	1960/11/15	1781	36	1981/10/12	9417	60	2001/04/15	16542
12	1960/11/20	1786	37	1982/11/26	9827	61	2001/04/18	16545
13	1961/07/18	2026	38	1982/12/08	9839	62	2001/11/04	16745
14	1961/07/20	2028	39	1984/02/16	10274	63	2001/12/26	16797
15	1966/07/06	3840	40	1989/07/25	12260	64	2002/08/24	17038
16	1967/01/28	4046	41	1989/08/16	12282	65	2003/10/28	17468
18	1968/09/29	4656	42	1989/09/29	12326	66	2003/10/29	17469
19	1968/11/18	4706	43	1989/10/19	12346	67	2003/11/02	17473
20	1969/02/25	4805	44	1989/10/22	12349	68	2005/01/17	17915
21	1969/03/30	4838	45	1989/10/24	12351	69	2005/01/20	17918
22	1971/01/24	5503	46	1989/11/15	12373	70	2006/12/13	18610
23	1971/09/01	5723	47	1990/05/21	12560	71	2012/05/17	20592
24	1972/08/04	6061	48	1990/05/24	12563	72	2017/09/10	22534
25	1972/08/07	6064	49	1990/05/26	12565	73	2021/10/28	24043
26	1973/04/29	6329	50	1990/05/28	12567	74	2024/05/11	24969
27	1976/04/30	7426	51	1991/06/11	12946	75	2024/06/08	24997
28	1977/09/19	7933	52	1991/06/15	12950	76	2024/11/21	25163
29	1977/09/24	7938	53	1992/06/25	13326	77	2025/11/11	25518

value is indeed remarkably close to the value of 1.723 years we had derived as the dominant beat of the tidally triggered magneto-Rossby waves.

In the following, two modifications will be applied. Firstly, we correct a timing error in [Stefani et al. \(2025\)](#) that led to an incorrect phase of $\varphi_0 = 1.88$, when it should have been $\varphi_0 = 2.19$. While this phase error (equivalent to a time shift of 31 days) had no effect on the main message of [Stefani et al. \(2025\)](#), it will be important later on when considering the predictability of the solar events of early 2026.

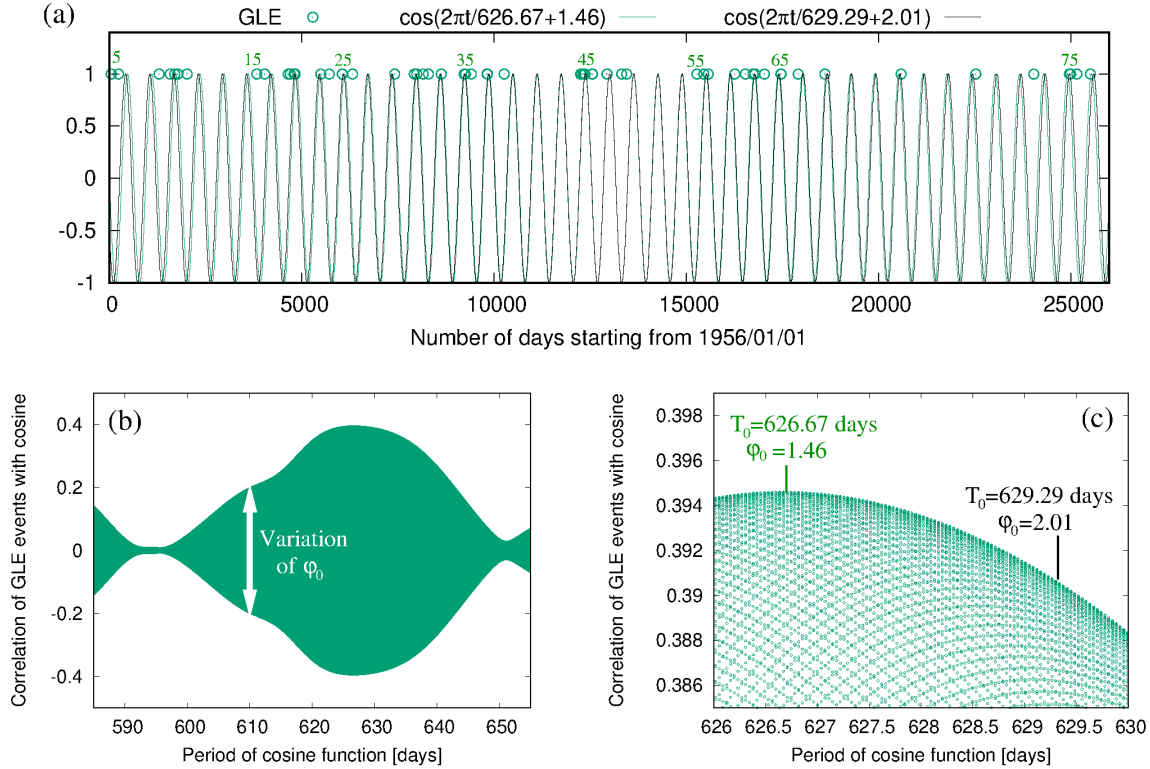


Figure 1. Analysis of GLE data. (a) Distribution of 72 events (green open circles) observed between 1956 February and 2025 November, as obtained from <https://gle.oulu.fi>. The abscissa shows the time t in days starting from 1956 January 1. A few event numbers according to Table 1 are indicated. The green curve shows the optimum cosine function $\cos(2\pi t/626.67 + 1.46)$ that maximizes the correlation coefficient given in Equation (1). The black curve displays $\cos(2\pi t/629.29 + 2.01)$ that results from the phase optimization when the theoretical period of $T_0 = 629.29$ days is fixed beforehand. (b) Correlation coefficient $Corr$ of the 72 GLE events with cosine functions with variable periods T_0 and phases φ_0 . For each period T_0 , the vertical extent emerges when using different phases φ_0 between 0 and 2π . (c) Zoomed-in version of (b), showing the maximum of $Corr$ appearing for $T_0 = 626.67$ days and $\varphi_0 = 1.46$. If the period is fixed beforehand to $T_0 = 629.29$ days, we obtain a slightly decreased correlation coefficient for an optimum $\varphi_0 = 2.01$. These periods and phases are used for defining the green and black curves in (a).

Secondly, from here on we will use a modified measure of correlation in the form

$$Corr = \frac{\sum_{i=1}^N \cos(2\pi t_i/T_0 + \varphi_0)}{\sqrt{\sum_{i=1}^N \cos^2(2\pi t_i/T_0 + \varphi_0)}} \quad (1)$$

which is closer in spirit to Pearson’s correlation coefficient between events (characterized by a number 1) and the underlying cosine function.

Table 1 lists the 72 GLE events between February 1956 and November 2025. The results of the data analysis are shown in Figure 1. Panel (a) displays the distribution of the 72 GLE events over time. Panels (b) and (c) illustrate the determination of the optimal period $T_0 = 626.67$ days and phase angle $\varphi_0 = 1.46$, which are used to define the green curve in panel (a). Additionally, we also determine the optimum phase when fixing T_0 beforehand to the theoretical value of 629.29 days as derived from the Rossby-wave theory. The resulting cosine function is displayed in black in panel (a). The two curves are almost indistinguishable from each other, with a mere 0.4 per cent difference in period. This suggests that the underlying theory may have some merit. Note also that the two correlation values obtained, 0.394 and 0.391, correspond to two-sided p -values of 0.0006 and 0.0007 for a sample size of 72, which indicates a high level of significance for the correlation. Admittedly, since Corr is not exactly a Pearson correlation coefficient, those p values should be interpreted with some caution.

3. S-CLASS FLARES

In this section we apply the methodology outlined in the previous section to the 37 events of solar superflares of S-class ($>\text{X}10$ in soft X-rays) that were recorded since 1978 (Tan et al. 2025). The occurrence of these S-flares was recently shown in the wavelet analysis of Velasco Herrera (2026) to be governed by coupled phase states of 1.7-year and 7-year oscillations. The dates of these events, taken from Tan et al. (2025); Velasco Herrera (2026), are listed in Table 2.

The data analysis is illustrated in Figure 2. Panel (a) shows the distribution of the 37 S-flare events, while in panels (b) and (c) the optimal periods T_0 and phase angles φ_0 are determined. Here, the best-fit period, $T_0 = 637.92$ days, is a bit farther away (1.4 per cent) from the theoretical value of 629.29 days. For $N = 37$, the two correlations of 0.72 for the optimum period of 1.747 years and 0.64 for the theoretical period of 1.723 years have p -values as low as 6×10^{-7} and 2×10^{-5} , respectively, which implies an even higher significance of the correlations than in the GLE case.

Table 2. Number, dates in the format YYYY/MM/DD, and days elapsed since 1955/12/31 of the 37 S-flare events considered here. The data are from [Tan et al. \(2025\)](#) and [Velasco Herrera \(2026\)](#).

Nr	Date	Days	Nr	Date	Days	Nr	Date	Days
1	1978/7/11	8228	14	1990/5/24	12563	27	2001/4/15	16542
2	1980/11/6	9077	15	1991/1/25	12809	28	2003/10/28	17468
3	1982/6/3	9651	16	1991/3/4	12847	29	2003/10/29	17469
4	1982/6/6	9654	17	1991/3/22	12865	30	2003/11/2	17473
5	1982/7/12	9690	18	1991/6/1	12936	31	2003/11/4	17475
6	1982/12/15	9846	19	1991/6/4	12939	32	2005/1/20	17918
7	1982/12/17	9848	20	1991/6/6	12941	33	2005/9/7	18148
8	1984/4/24	10342	21	1991/6/9	12944	34	2006/12/5	18602
9	1984/5/20	10368	22	1991/6/11	12946	35	2011/8/9	20310
10	1989/3/6	12119	23	1991/6/15	12950	36	2017/9/6	22530
11	1989/8/16	12282	24	1992/11/2	13456	37	2017/9/10	22534
12	1989/9/29	12326	25	1997/11/6	15286	-	-	-
13	1989/10/19	12346	26	2001/4/2	16529	-	-	-

4. GLE AND S-FLARE EVENTS TAKEN TOGETHER

Given the very close results obtained for the best-fit periods of the 72 GLE events and the 37 S-flares, we decided to assess also a combined dataset of 109 events in total. This is shown in Figure 3. Here, the resulting best-fit period, $T_0 = 632.88$ days, is only 0.6 per cent away from the theoretical value of 629.29 days. For $N = 109$, the two correlations of 0.435 for the optimum period 1.733 years and 0.424 for the theoretical period of 1.723 years have p-values of 4×10^{-6} and 6×10^{-6} , respectively.

While all previous analyses used simple cosines as test functions, in the following we move closer to the Rossby-wave mechanism underlying the synchronization theory of the solar dynamo that we have developed over the last decade ([Weber et al. 2015](#); [Stefani et al. 2016, 2019, 2021](#); [Klevs et al. 2023](#); [Horstmann et al. 2023](#); [Stefani et al. 2024, 2025](#)), building on previous work of [Abreu et al. \(2012\)](#); [Scafetta \(2012\)](#); [Wilson \(2013\)](#); [Okhlopkov \(2016\)](#).

Following [Stefani et al. \(2025\)](#), we consider the sum of three tidal wave excitations with periods of (approximately) 118 days, 199 days and 292 days that correspond to the two-planet spring-tides of Venus-Jupiter, Earth-Jupiter and Venus-Earth, respectively:

$$s(t) = \cos \left(2\pi \cdot \frac{t - t_{VJ}}{0.5 \cdot P_{VJ}} \right) + \cos \left(2\pi \cdot \frac{t - t_{EJ}}{0.5 \cdot P_{EJ}} \right) + \cos \left(2\pi \cdot \frac{t - t_{VE}}{0.5 \cdot P_{VE}} \right). \quad (2)$$

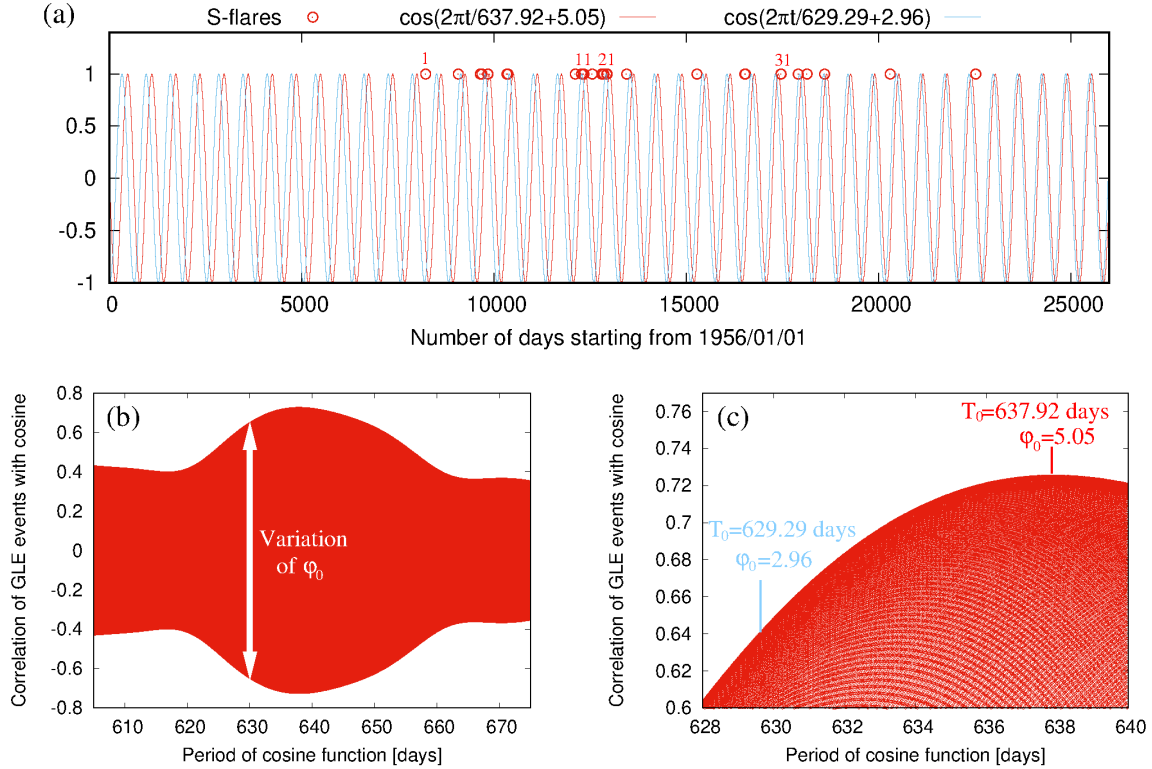


Figure 2. Same as Figure 1, but for the 37 S-flare events since 1978. Here, the red curve shows the optimum cosine function $\cos(2\pi t/637.92 + 5.05)$ that maximizes Corr given in Equation (1). The light blue curve shows $\cos(2\pi t/629.29 + 2.96)$ that results from the optimization of the phase when the theoretical period of $T_0 = 629.29$ days is fixed beforehand.

To be more specific, we use the accurate two-planet synodic periods $P_{\text{VJ}} = 0.64884$ years, $P_{\text{EJ}} = 1.09207$ years, $P_{\text{VE}} = 1.59876$ years, and the epochs of the corresponding conjunctions $t_{\text{VJ}} = 2002.34$, $t_{\text{EJ}} = 2003.09$, and $t_{\text{VE}} = 2002.83$ that were adopted from [Scafetta & Bianchini \(2022\)](#).

While this sum of the three tidal forcings might already be important for the excitation of tachocline deformations and the launching of flux tubes ([Dikpati & McIntosh 2020](#)), in the following we consider its square which may be more relevant for nonlinear tachocline oscillations, modifications of zonal or meridional flows, or the wave-related helicity and α -effect.

The square $s^2(t)$ of the sum of the three cosine functions is shown as the dark blue curve in panels (a) and (b) of Figure 4, together with the 72 GLE and 37 S-flare events. Compared to Figures 1, 2, 3, we have doubled the time-resolution in order to better recognize the frequent (although not perfect) coincidences of solar events with the spikes of $s^2(t)$. While the average distance between these spikes

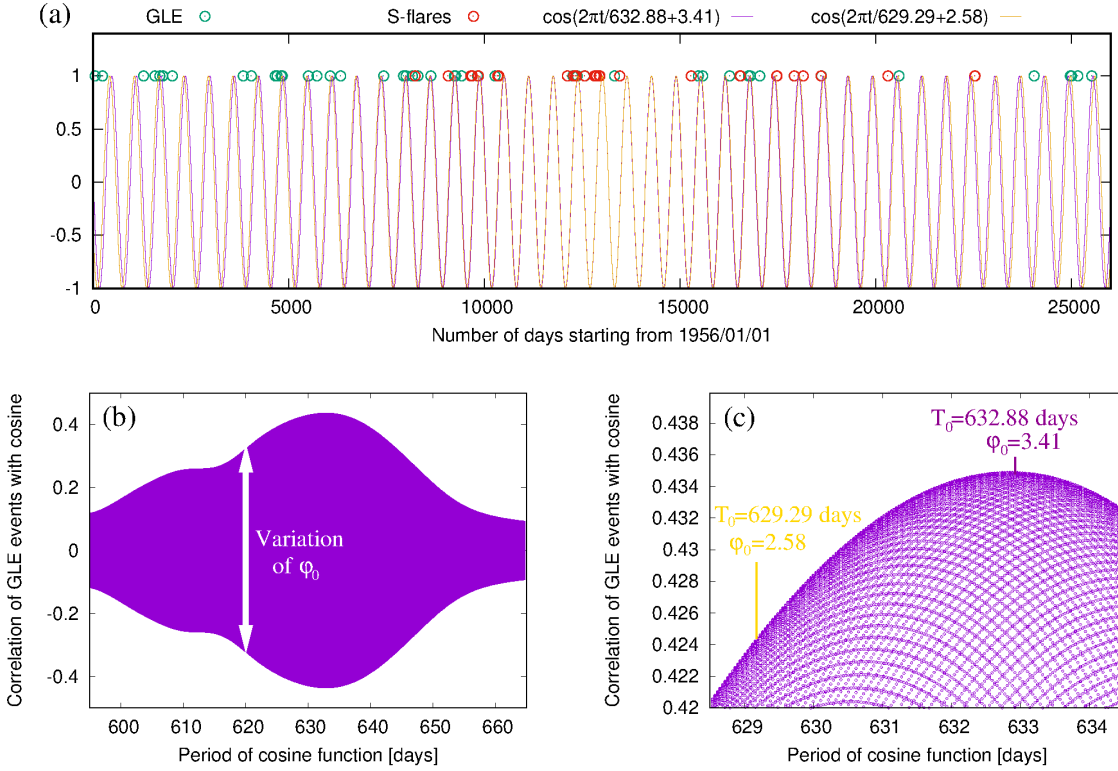


Figure 3. Same as Figure 1, but for the merger of the 72 GLE (green open circles) with the 37 S-flare events (red open circles). Here, the violet curve shows the optimum cosine function $\cos(2\pi t/632.88 + 3.41)$. The gold curve shows $\cos(2\pi t/629.29 + 2.58)$ that results from the optimization of the phase when the theoretical period of $T_0 = 629.29$ days is fixed beforehand.

corresponds to the above-mentioned beat period of 1.723 years (629.29 days), they show a systematic oscillation leading to the additional 11.07-year beat period which can be recognized in the changing height of the spikes. As an aside, this second period is at the root of our parametric resonance model to describe the Schwabe cycle (Stefani et al. 2019; Klevs et al. 2023; Stefani et al. 2024, 2025).

In the following we will assess the correlation of the tidal forcing $s^2(t)$ with the solar events which is defined, in analogy to Equation (1), as

$$\text{Corr} = \frac{\sum_{i=1}^N [s^2(t_i) - \bar{s^2(t)}]}{\sqrt{\sum_{i=1}^N [s^2(t_i) - \bar{s^2(t)}]^2}}. \quad (3)$$

For that it will also be useful to “smear out” the very spiky shape of $s^2(t)$ by applying to it a moving average with different window lengths. Three of those curves are displayed in panels (a) and (b) of Figure 4 with different colors. For the original $s^2(t)$ and the three time-averages we ask now which

time-shift (backward or forward) would give the highest correlation with the solar event data. While this basically corresponds to the phase optimization for the single cosine functions as carried out in Figures 1, 2, and 3, now the time-shift has a clear physical meaning in that it describes the lag between the maximum tidal triggering of Rossby waves and the solar event that ultimately occurs at the solar surface. In view of the typical rise times of flux tubes in the order of a month or more (Weber et al. 2011), one would expect a similar time lag to come out as a sort of optimum.

However, the picture arising from panels (c) and (d) of Figure 4 is less clear. While in general the correlation peaks around zero time lag, in particular the dark blue curve of $s^2(t)$ has a somewhat counterintuitive peak at a *positive* time shift of approximately 60 days with respect to the solar events. For longer time averages (yellow and gold), the correlation curves become much smoother and indeed peak around a zero time lag.

What is remarkable in this respect is the case of an average window of 101 days. For this window length the main peaks in panels (a) and (b) come to lie in between the peaks of the original signal $s^2(t)$. A similar effect of the averaging was already observed in Stefani et al. (2025) for the 11.07-year beat period. We will later come back to this point when discussing the Carrington event.

5. X-FLARE OF 2026 FEBRUARY 1

The high solar activities of early 2026 occurred approximately 1.7 years after the two GLE's of 2024 May and June. In this section, we will assess the possible connection between these events and the strong tidal forcings resulting from the alignment of Venus, Earth and Jupiter.

To start with, we display in Figure 5(a) the X8.3-class flare of 2026 February 1 (red full triangle) in the context of the solar events since late 1977 November (8000 days after 1956/01/01). We also plot $s^2(t)$, alongside the black, light blue and gold curves from Figures 1, 2 and 3, which had come out as the best fits when the period was fixed beforehand to 629.29 days. Obviously, all these curves are very close to each other, and the spiky $s^2(t)$ curve fits nicely into the picture, despite its slight wiggling to the left and right associated with the occurrence of double peaks. Overall, we also observe a significant, albeit not perfect, synchronism between the peaks of the four curves and the solar events.

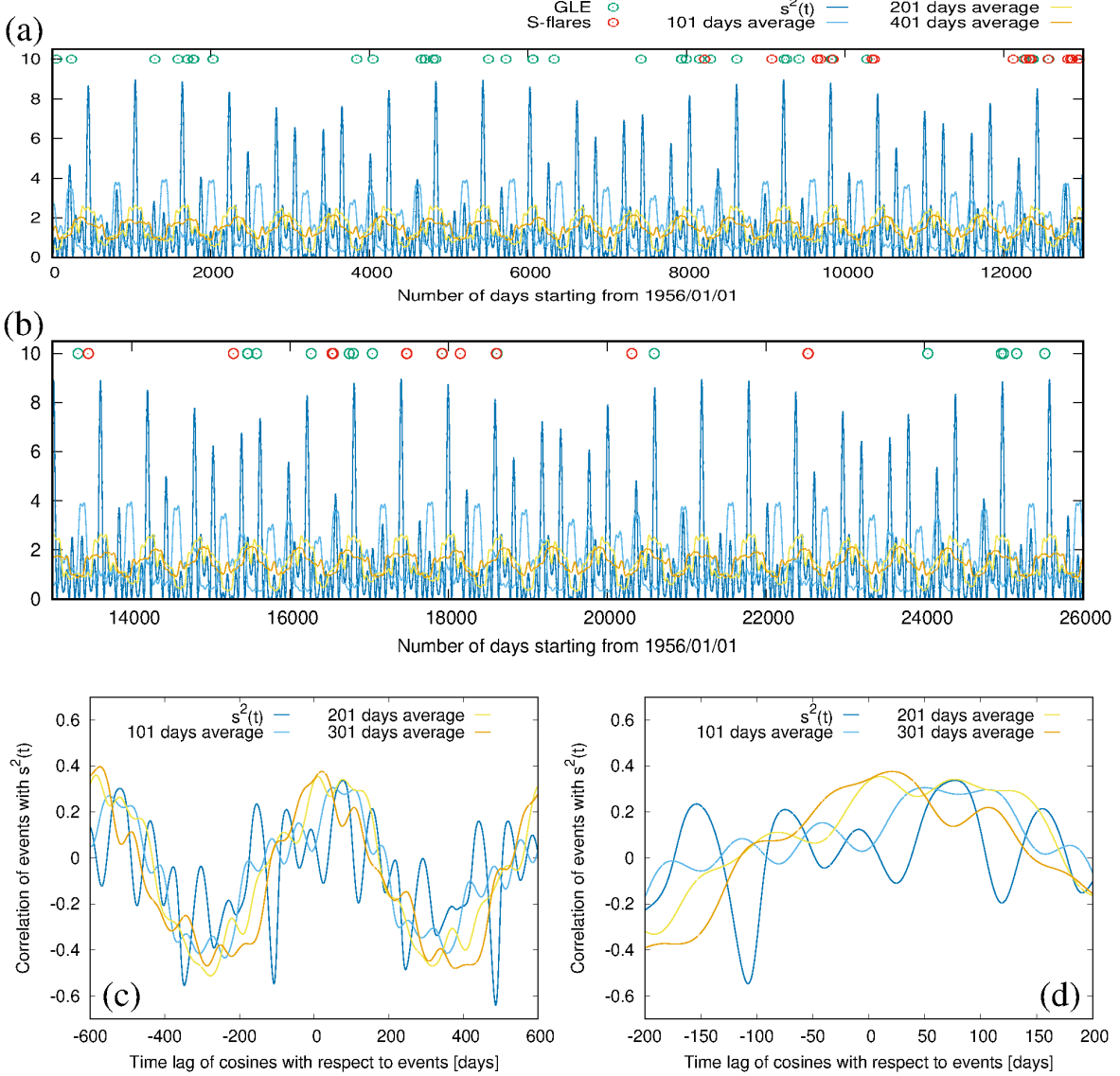


Figure 4. GLE and S-flare events, $s^2(t)$, and different time averages of it (a,b). The longer beat period of 11.07 years (corresponding to the Schwabe cycle) can be recognized in the varying height of the spikes. Correlation coefficients of the four curves from (a,b) with the solar events in dependence on the time lag (c). The same, but zoomed in on shorter time lags (d).

The focus in panel (b) of Figure 5 is now on the last two years. On the left-hand side, we recognize the two GLE events that occurred on 2024 May 11 and 2024 June 8. Remarkably, the peak of $s^2(t)$ lies almost exactly between these two closely neighboring events. Very close to it lies the black curve, representing the best-fit of the GLE events for the fixed 629.29-day period. The other two curves (the light blue and gold ones) are shifted slightly towards earlier times. Turning to the right-hand

side of panel (b), we see that the strong X-flare event of 2026 February 1 occurred only 23 days after the peak of $s^2(t)$ located on 2026 January 9. The dates of the maxima of the pure cosines are also displayed. Note that the sequence of the maxima of the dark blue and the black curve has interchanged between 2024 and 2026. While both have the same dominant period of 629.29 days, $s^2(t)$ has slightly wiggled to the left.

In panel (c) we show the corresponding green, red and violet single-cosine curves from Figures 1, 2, 3 which were obtained when optimizing both the phases *and* the periods. Once again, we see a fairly good correlation with the solar events.

Finally, let us take a look at the dashed and dotted green curves in panel (c). The dotted one, $\cos(2\pi t/629.85 + 1.88)$, was presented in [Stefani et al. \(2025\)](#) as the best fit when using the simplified correlation expression $\text{Corr} = 1/71 \sum_{i=1}^{71} \cos(2\pi t_i/T_0 + \phi_0)$. However, this solution was flawed due to a bug in the code, and it should have been the dashed green curve, i.e. $\cos(2\pi t/629.85 + 2.19)$. The 31-day difference between them explains the inaccuracy of the forecast made on 7 January 2026, as mentioned above. In any case, in view of the results obtained in the present paper, we would generally argue in favour of using the maximum of $s^2(t)$ for any forecasting purposes. Indeed, both the two GLE events of 2024 and the strong X-flare of 2026 February 1 occurred very close to the peaks of $s^2(t)$. The timing of the latter event aligns closely with the expected one-month lag for the flux tubes to emerge on the Sun’s surface ([Weber et al. 2011](#)), although this may be a coincidental occurrence.

6. WHAT ABOUT CARRINGTON?

Encouraged by the highly significant correlations between the peaks of the three tidal forcings and the 72 GLE events and 37 S-class flares, this section examines whether the Carrington event of 1859 September 1 could be “postdicted”. As shown in Figure 6, this date corresponds to 35,185 days before 1956 January 1. While the Carrington event occurred during the rising flank of solar cycle 10 (whose maximum lied in February 1860), its date falls rather precisely between two peaks of the $s^2(t)$ curve. This indicates that, although there is a strong *statistical* correlation between solar activity and the tidal triggers of magneto-Rossby waves, it is not possible to predict every single event in a

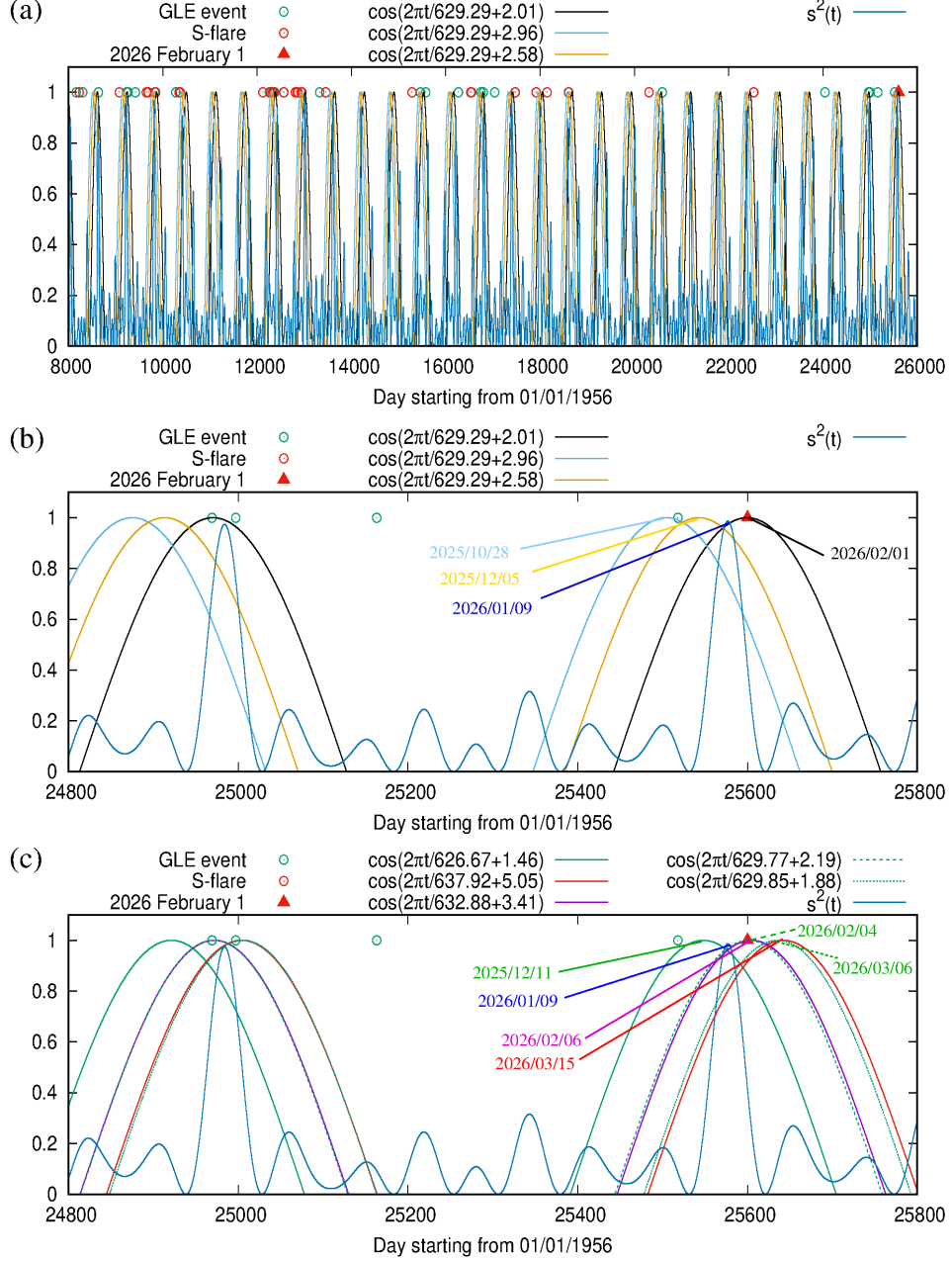


Figure 5. The 2026 February 1 event and its potential predictability. (a) GLE and S-flare events since 1977 November together with $s^2(t)$ and the three optimized 629.29-day periodic functions. The strong X-flare of 2026 February 1 is added as a red triangle. (b) Details of (a) with the dates of the maxima of the four curves indicated. (c) Modification of (b) showing the curves with optimized phases φ_0 and periods T_0 . The dashed green curve with $\varphi_0 = 2.19$ would result when using the correlation function without denominator. The dotted green line, with the erroneous phase $\varphi_0 = 1.88$, was given in Stefani et al. (2025). The phase difference corresponds to the time shift of 31 day by which the prediction for the early 2026 events was off.

deterministic manner. To some extent, however, this was already evident when examining the details of Figure 4, where several events did not correspond to beat maxima.

Another issue that arises at this point is the shift in the maximum that occurs when certain time averages are applied, as mentioned above in the discussion of Figure 4. It might therefore be worth checking whether the Carrington event and other events that do not occur close to the peaks of $s^2(t)$ can be explained in this way.

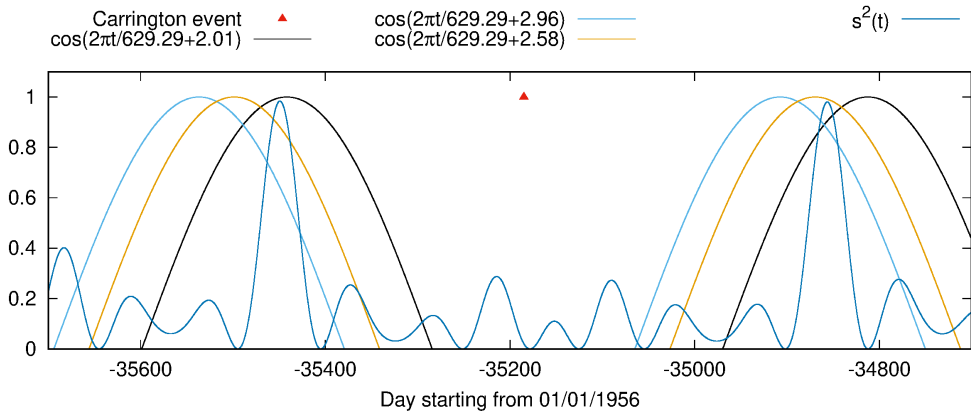


Figure 6. The Carrington event of 1859 September 1, situated quite in the middle between the two neighboring peaks of the tidal forcing curve $s^2(t)$.

7. CONCLUSIONS

In this paper we have refined and deepened our previous examination of a potential link between extreme solar events with tidal triggers of magneto-Rossby waves at the solar tachocline. As for the GLE events, we found a correlation coefficient of 0.394 when using a cosine function with an optimized period of 1.716 years. Utilizing the theoretical beat period of 1.723 years gave a slightly reduced value of 0.391. For the 72 GLE events used, the corresponding low p-values pointed to a high significance of the correlations.

When applying the same method to the sequence of 37 S-class flares, we found even higher correlations of 0.72 and 0.64 for the optimized and theoretical periods of 1.747 and 1.723 years, respectively. The corresponding p-values were very low.

We also applied the method to a simple merger of the GLE and S-flare events. For the arising 109 events we obtained correlations of 0.434 for an optimum period of 1.733 years and 0.424 for 1.723 years, leading again to rather low p-values of 4×10^{-6} and 6×10^{-6} , respectively.

Optimizing the functions with fixed periods for different data sets results in a 15 per cent difference in phase, equivalent to 95 days. This, along with the highly significant correlations, indicates a phase-stable process that governs solar activity.

For the merged data set, we also computed the correlation of the events with the square of the sum of the three tidal trigger functions which is dominated by steep peaks separated, on average, by gaps of 629.29 days (1.723 years). When shifting this function (and its various moving averages) backwards or forwards in relation to the solar events, we found that the maximum correlation typically occurred with a positive time shift of up to 70 days. At first glance, this is surprising, since one would expect the reverse, meaning that tidal peaks should precede solar events. One possible explanation is the significant width (of approximately 100 days) of the main peaks of the $s^2(t)$ curve, which could induce flux tube launches already at the rising flank of the tidal trigger of the Rossby waves. In view of the oscillatory behavior of the $s^2(t)$ curve, such a high sensitivity could perhaps also explain the occurrence of solar events in between the spikes, as was strikingly evident for the Carrington event.

All this shows that we still have a long way to go before we understand the physical mechanism that links the excitation of magneto-Rossby waves by tides with the launching of flux tubes. It goes without saying that any viable forecast must also take into account the current phase of the 11-year Schwabe cycle. In this context, the third harmonic of the Hale cycle may also play a role, as suggested by recent results of [Velasco Herrera \(2026\)](#). Apart from this, we must also acknowledge that although Rossby waves provide an ideal resonance ground for tidal forces to act upon, it cannot be ruled out that other mechanisms are at play.

In the future, it may also be worthwhile including somewhat less extreme events, such as X-flares and sub-GLE events, in the data analysis.

ACKNOWLEDGMENTS

This work received funding from the Helmholtz Association in frame of the AI project GEOMAGFOR (ZT-I-PF-5-200). F. S. thanks Willie Soon for providing an early version of [Velasco Herrera \(2026\)](#), which shows evidence of a 1.7-year signal in S-flare data. He would also like to thank Lakshmi Pradeep Chitta for an inspiring discussion about the “postdictability” of the Carrington event and Tony Phillips for enquiring into potential impacts of the January 2026 alignment on solar activity.

REFERENCES

Abreu, J. A., Beer, J., Ferriz-Mas, A., McCracken, K. G., & Steinhilber, F. 2012, *A&A*, 548, 9, doi: [10.1051/0004-6361/201219997](https://doi.org/10.1051/0004-6361/201219997)

Dikpati, M. 2012, *ApJ*, 745, 128, doi: [10.1088/0004-637X/745/2/128](https://doi.org/10.1088/0004-637X/745/2/128)

Dikpati, M., & McIntosh, S. W. 2020, *Space Weather*, 18, e2018SW002109, doi: [10.1029/2018SW002109](https://doi.org/10.1029/2018SW002109)

Dikpati, M., McIntosh, S. W., Bothun, G., et al. 2018, *The Astrophysical Journal*, 853, 144, doi: [10.3847/1538-4357/aaa70d](https://doi.org/10.3847/1538-4357/aaa70d)

Horstmann, G. M., Mamatsashvili, G., Giesecke, A., Zaqrashvili, T. V., & Stefani, F. 2023, *The Astrophysical Journal*, 944, doi: [10.3847/1538-4357/aca278](https://doi.org/10.3847/1538-4357/aca278)

Klevs, M., Stefani, F., & Jouve, L. 2023, *Solar Physics*, 298, doi: [10.1007/s11207-023-02173-y](https://doi.org/10.1007/s11207-023-02173-y)

Márquez-Artavia, X., Jones, C. A., & Tobias, S. M. 2017, *Geophysical & Astrophysical Fluid Dynamics*, 111, 282, doi: [10.1080/03091929.2017.1301937](https://doi.org/10.1080/03091929.2017.1301937)

Okhlopkov, V. P. 2016, *Moscow Univ. Phys. Bull.*, 71, 440, doi: [10.3103/S0027134916040159](https://doi.org/10.3103/S0027134916040159)

Pedlosky, J. 1987, *Geophysical Fluid Dynamics*, 2nd edn. (New York: Springer-Verlag), doi: [10.1007/978-1-4612-4650-3](https://doi.org/10.1007/978-1-4612-4650-3)

Raphaldini, B., & Raupp, C. F. M. 2015, *The Astrophysical Journal*, 799, 78, doi: [10.1088/0004-637X/799/1/78](https://doi.org/10.1088/0004-637X/799/1/78)

Rossby, C.-G. 1939, *J. Mar. Res.*, 2, 38

Scafetta, N. 2012, *Journal of Atmospheric and Solar-Terrestrial Physics*, 81-82, 27, doi: [10.1016/j.jastp.2012.04.002](https://doi.org/10.1016/j.jastp.2012.04.002)

Scafetta, N., & Bianchini, A. 2022, *Frontiers in Astronomy and Space Sciences*, 9, 937930, doi: [10.3389/fspas.2022.937930](https://doi.org/10.3389/fspas.2022.937930)

Stefani, F., Giesecke, A., Weber, N., & Weier, T. 2016, *Solar Physics*, 291, 2197, doi: [10.1007/s11207-016-0968-0](https://doi.org/10.1007/s11207-016-0968-0)

Stefani, F., Giesecke, A., & Weier, T. 2019, *Solar Physics*, 294, 60, doi: [10.1007/s11207-019-1447-1](https://doi.org/10.1007/s11207-019-1447-1)

Stefani, F., Horstmann, G. M., Klevs, M., Mamatsashvili, G., & Weier, T. 2024, Solar Physics, 299, doi: [10.1007/s11207-024-02295-x](https://doi.org/10.1007/s11207-024-02295-x)

Stefani, F., Horstmann, G. M., Mamatsashvili, G., & Weier, T. 2025, Solar Physics, 300, doi: [10.1007/s11207-025-02521-0](https://doi.org/10.1007/s11207-025-02521-0)

Stefani, F., Stepanov, R., & Weier, T. 2021, Solar Physics, 296, 88, doi: [10.1007/s11207-021-01822-4](https://doi.org/10.1007/s11207-021-01822-4)

Tan, B., Zhang, Y., Huang, J., & Ji, K. 2025, ASTROPHYSICAL JOURNAL LETTERS, 979, doi: [10.3847/2041-8213/ada611](https://doi.org/10.3847/2041-8213/ada611)

Velasco Herrera, V. M., Perez-Peraza, J., Soon, W., & Marquez-Adame, J. C. 2018, New Astronomy, 60, 7, doi: [10.1016/j.newast.2017.09.007](https://doi.org/10.1016/j.newast.2017.09.007)

Velasco Herrera, V. M. e. a. 2026, JGR: Space Physics, in press

Weber, M. A., Fan, Y., & Miesch, M. S. 2011, Astrophysical Journal, 741, doi: [10.1088/0004-637X/741/1/11](https://doi.org/10.1088/0004-637X/741/1/11)

Weber, N., Galindo, V., Stefani, F., & Weier, T. 2015, New J. Phys., 17, 113013, doi: [10.1088/1367-2630/17/11/113013](https://doi.org/10.1088/1367-2630/17/11/113013)

Wilson, I. R. G. 2013, Pattern Recognition in Physics, 1, 147, doi: [10.5194/prp-1-147-2013](https://doi.org/10.5194/prp-1-147-2013)

Zaqarashvili, T. V., Carbonell, M., Oliver, R., & Ballester, J. L. 2010a, ApJL, 724, L95, doi: [10.1088/2041-8205/724/1/L95](https://doi.org/10.1088/2041-8205/724/1/L95)

—. 2010b, ApJ, 709, 749, doi: [10.1088/0004-637X/709/2/749](https://doi.org/10.1088/0004-637X/709/2/749)

Zaqarashvili, T. V., Albekioni, M., Ballester, J. L., et al. 2021, Space Sci Rev, 217, 15, doi: [10.1007/s11214-021-00790-2](https://doi.org/10.1007/s11214-021-00790-2)